# On a Chirplet Transform based method applied to separating and counting wolf howls [1]

B. Dugnol, C. Fernández, G. Galiano [2] and J. Velasco

*Dpto. de Matemáticas, Universidad de Oviedo, c/ Calvo Sotelo, 33007-Oviedo Spain*

**Abstract**

We propose a parametric model based in chirp decomposition to modelize wolf chorus emissions. The problem consists on estimating the phase and amplitude of chirps corresponding to each individual, as well as the number of individuals. For the first task, we use a well known technique, the Chirplet Transform, which allows us to obtain a first order approximation of the phase, improving the zero order approximation given by the Short Time Fourier Transform (STFT). This gain in accuracy allows to use criteria for a better chirp tracking, which is specially important at crossing points and in the determination of harmonics of a fundamental tone. We explore the efficiency of the method applying it to synthetic signals and to wolves choruses recordings (original motivation of this work). The results show good performance for chirps tracking even under strong noise corruption.

*Key words:* Chirp transform, instantaneous frequency estimation, parametric method, voice separation, multiple instantaneous frequency tracking, population counting.

## 1 Introduction

It is well known the social controversy caused by wolf in most of the countries they are present. On one hand, in very populated regions, such as Europe, they compete with human both for space and natural resources, causing, in many

[1] All the authors are partially supported by Project PC0448, Gobierno del Principado de Asturias, Spain. Third and fourth authors are partially supported by the Spanish DGI Project MTM2004-05417.

[2] Corresponding author. Phone:+34 985182299 Fax: +34 985103354

[3] dugnol@uniovi.es, carlos@uniovi.es, galiano@uniovi.es, julian@uniovi.es

occasions, damages and costs to human interests, mainly through attacks to livestock. On the other hand, due to extinction risk, wolf is a protected specie around the world, being the costs they produce usually charged to public budgets. Hence, it is a common interest to scientists and authorities to estimate their populations. However, estimating wolf population is a difficult task which, traditionally, relies either on the recuperation of field traces, such as steps on the snow, or in the direct observation of wolf packs. The efficiency of these methods is quite variable, depending on the specific habitat of interest (existence of regular and long-lasting snowfalls, orographic characteristics of the region, etc). As a complement to traditional techniques, we present in this article a method based in Signal Theory to extract information about wolf populations of a given area from field recordings of their choruses. In previous papers [1,2] we dealt with the first step of our technique: denoising and enhancing the signals contained in recordings made, usually, in adverse situations. In the present work, we study the utilization of a parametric model together with the Chirplet Transform to extract the relevant information (howls and barks) from the denoised recordings and give, after a suitable processing of the signal, an estimation of the number of individuals emitting in such recording.

In our numerical experiments we use wolves choruses signals recorded both in wilderness and in captivity [3,4]. The objective is to separate the different howls composing the chorus and therefore may be considered as a source separation problem. The literature on this subject is broad, ranging from simpler situations like the $n$-microphone $n$-sources separation problem to more complex analysis such as the one-microphone blind source separation problem [5–7]. Our problem is placed somewhere in between since it is a one-microphone multi-source separation problem, but it is not of a blind nature since a parametric representation based on a chirp decomposition of the signal seems to be reasonable for the wolf howls modeling.

## 2 Howl tracking and separation

A wolves chorus is composed, mainly, by howls and barks which, from the analytical point of view, may be regarded as chirp functions. The former has a long time support and a small frequency range variation, while the latter is almost punctually localized in time but posses a large frequency spectrum. It is convenient, therefore, adopting a parametric model to represent the wolves chorus as an addition of chirps given by the function $f : [0, T] \to \mathbb{C}$,

$$f(t) = \sum_{n=1}^{N} a_n(t) \exp[i\phi_n(t)], \tag{1}$$

with $T$ the length of the chorus emission, $a_n$ and $\phi_n$ the chirps amplitude and phase, respectively, and with $N$, the number of chirps contained in the chorus. We notice that $N$ is not necessarily the number of wolves since, for instance, harmonics of a given fundamental tone are counted separately.

To identify the unknowns $N$, $a_n$ and $\phi_n$ we proceed in two steps. Firstly, for a discretization of the time interval $[0, T]$, say $t_k = k * \tau$, for the time step $\tau > 0$ and $k = 0, \ldots, K$, we produce estimates of the amplitude $a_n(t_k)$ and the phase $\phi_n(t_k)$ of the chirps contained at such discrete times. Secondly, we establish criteria which allow us deciding if the computed estimates at adjacent times do belong to the same global chirp or do not. We shall describe the first step in the present section and postpone the treatment of the second step to the section of numerical experiments.

There exist a variety of methods for estimating the amplitude and phase of a given signal, most of them relying in the previous estimation of its instantaneous frequency (IF), $\phi'(t)$ [8–15]. However, since in our problem we are facing difficulties such as tracking the chirps at crossing points or identifying harmonics of a given fundamental chirp, it is convenient approximating the phase with more accuracy than just the first order IF estimation. The main tools available in the literature to jump to a second order chirp rate estimation are those based either in the Chirplet Transform [16,17], that we use in this article, or in the Fourier Fractional Transform [18,19]. The Chirplet Transform of a function $f \in L^2(\mathbb{R})$ is defined as

$$\Psi f\,(t_o, \xi, \mu; \lambda) = \int_{-\infty}^{\infty} f\,(t)\,\overline{\psi_{t_o,\xi,\mu,\lambda}\,(t)}dt, \tag{2}$$

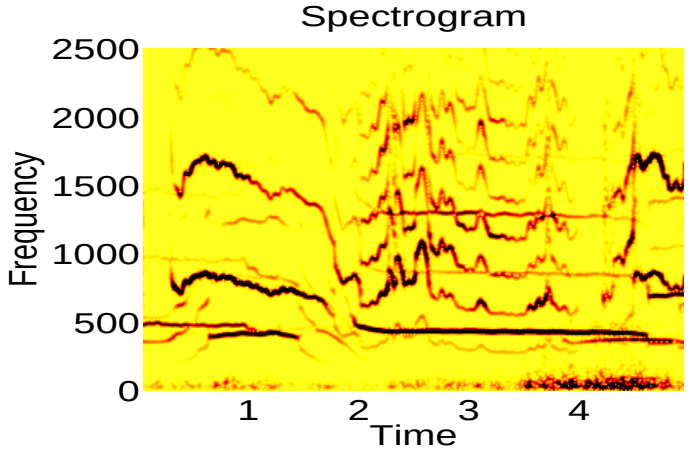


Fig. 1. A field recorded signal containing several multi-harmonic howls and barks together with a strong background noise.

with the complex window $\psi_{t_o,\xi,\mu,\lambda}$ given by

$$\psi_{t_o,\xi,\mu,\lambda}(t) = v_\lambda(t-t_o)\exp\left[i(\xi t + \frac{\mu}{2}(t-t_o)^2)\right]. \tag{3}$$

Here, $v \in L^2(\mathbb{R})$ denotes a non-negative, symmetric and normalized real window, and $v_\lambda(\cdot) = v(\cdot/\lambda)/\sqrt{\lambda}$, for $\lambda > 0$, and the parameters $t_o, \xi, \mu \in \mathbb{R}$, stand for time, IF and chirp rate, respectively. Observe that

$$\begin{aligned}\Psi f(t_o,\xi,\mu,\lambda) &= \int_{-\infty}^{\infty} f(t)\, v_\lambda(t-t_o)\exp\left[-i(\xi t + \frac{\mu}{2}(t-t_o)^2)\right]dt = \\ &= \int_{-\infty}^{\infty} \widetilde{f_{\lambda,t_o}}(x)\exp\left[-i\left(\xi x + \frac{\mu}{2}x^2\right)\right]dx,\end{aligned}$$

and therefore the chirp-linear transform provides a measure of the degree of correlation between the linear chirp, $\exp\left[-i\left(\xi x + \frac{\mu}{2}x^2\right)\right]$, and the portion of the signal centered at $t_o$, $\widetilde{f_{\lambda,t_o}}(x) = f(x+t_o)\, v_\lambda(x)\exp[-i\xi t_o]$. It is, then, clear (and straightforward to prove) that for a linear chirp of the form

$$f(t) = a(t)\exp[i(\frac{\alpha}{2}(t-t_o)^2 + \beta(t-t_o) + \gamma)],$$

and for fixed $t_0$ and $\lambda$, the quadratic energy distribution $\Psi f(t_0,\cdot,\cdot;\lambda)$ has a global maximum at $(\alpha,\beta)$, allowing us to determine the IF and chirp rate of a given linear chirp at a fixed time by computing the maximum point of the energy distribution. For more general forms of mono-component chirps we have the following localization result

**Theorem 1** *Let $f(t) = a(t)\exp[i\phi(t)]$, with $a \in L^2(\mathbb{R})$ non-negative and $\phi \in C^3(\mathbb{R})$. For all $\varepsilon > 0$ and $\xi, \mu \in \mathbb{R}$ there exists $L > 0$ such that if $\lambda < L$ then*

$$P_\Psi f(t_o,\xi,\mu;\lambda) \leqslant \lambda\varepsilon + P_\Psi f(t_o,\phi'(t_o),\phi''(t_o);\lambda). \tag{4}$$

*In addition,*

$$\lim_{\lambda\to 0}\frac{1}{\lambda}P_\Psi f(t_o,\phi'(t_o),\phi''(t_o);\lambda) = a(t_o)^2. \tag{5}$$

In other words, for a general mono-component chirp the energy distribution maximum provides an arbitrarily close approximation to the IF and chirp rate of the signal. Moreover, its amplitude may also be estimated by shrinking the window time support at the maximum point.

**Proof.** Consider the second order Taylor expansion of $\Psi f$ on $t_o$,

$$\phi(t) = \phi(t_o) + \phi'(t_o)(t-t_o) + \frac{1}{2}\phi''(t_o)(t-t_o)^2 + R_{t_o}(t),$$

with $\lim_{t\to t_o} R_{t_o}(t) = 0$. We have

$$|\Psi f\left(t_o, \phi'\left(t_o\right), \phi''\left(t_o\right), \lambda\right)| = \left|\int_{-\infty}^{\infty} a\left(t\right) v_\lambda(t - t_o) \exp\left[iR_{t_o}\left(t\right)\right] dt\right|,$$

and we deduce (5) using that

$$\lim_{\lambda\to 0} \frac{v_\lambda(t)}{\sqrt{\lambda}} = \delta\left(t\right). \tag{6}$$

To prove (4) we use the non-negativity of $a$ and $v$ to get

$$|\Psi f\left(t_o, \xi, \mu, \lambda\right)| \leqslant \int_{-\infty}^{\infty} a\left(t\right) v_\lambda(t - t_o) dt = \left|e^{i(\phi(t_o) - \phi'(t_o)t_o)} \int_{-\infty}^{\infty} a\left(t\right) v_\lambda(t - t_o) dt\right|. \tag{7}$$

Multiplying (7) by $1/\sqrt{\lambda}$, adding and subtracting $\Psi f\left(t_o, \phi'\left(t_o\right), \phi''\left(t_o\right), \lambda\right)/\sqrt{\lambda}$ inside the absolute value of the right hand side of (7) and using the triangle inequality we deduce

$$\begin{aligned}\frac{1}{\sqrt{\lambda}} |\Psi f\left(t_o, \xi, \mu, \lambda\right)| \leqslant &\left|e^{i(\phi(t_o) - \phi'(t_o)t_o)} \int_{-\infty}^{\infty} a\left(t\right) \frac{v_\lambda(t - t_o)}{\sqrt{\lambda}} (1 - \exp(iR_{t_o}\left(t\right))) dt\right| \\ &+ \frac{1}{\sqrt{\lambda}} \left|\Psi f\left(t_o, \phi'\left(t_o\right), \phi''\left(t_o\right), \lambda\right)\right|.\end{aligned}$$

But, again as a consequence of (6), we have

$$\int_{-\infty}^{\infty} a\left(t\right) \frac{v_\lambda(t - t_o)}{\sqrt{\lambda}} (1 - \exp(iR_{t_o}\left(t\right))) dt \to 0,$$

as $\lambda \to 0$. The assertion follows. ■

Finally, for a multi-component chirp $f\left(t\right) = \sum_{n=1}^{N} a_n\left(t\right) \exp[i\phi_n\left(t\right)]$ the situation is somehow more involved since although the energy distribution still has maxima at $\left(\phi_n'\left(t_o\right), \phi_n''\left(t_o\right)\right)$ for all $n$ such that $a_n\left(t_o\right) \neq 0$, these are now of local nature, and in fact, spurious local maxima not corresponding to any chirp may appear due to the energy interaction among the actual chirps.

## 3 Numerical experiments

In this section, we present some results obtained with the algorithm described in the previous section when applied to both synthetic and wolves choruses field recorded signals.

In the first part of Experiment 1, we process a clean synthetic signal composed by three nonlinear chirps with multiple crossings. The computation of

IF, chirp rate and amplitude approximations is very accurate and allows us to separate the three chirps in their whole time support. In the second part of this experiment, we add to the previous signal a Gaussian noise of the same amplitude, i.e., with signal to noise ratio, SNR=0. We perform here two computations. Firstly, we use the Chirp Transform directly to the signal for the chirp separation. We observe that the algorithm is still capable of separating the main (higher amplitude) pieces of the three chirps. However, noise corruption affects to the chirp identification of the low amplitude segments of the signal, avoiding the recognition of these segments. Consequently, we restart the analysis of the noisy signal by filtering it in advance with the noise reduction signal enhancement algorithm described in [2], and then use the Chirp Transform based algorithm for separating the resulting signal. In this case, the low amplitude tails of the original signal are captured more accurately, although the computational cost is significantly increased.

The last two experiments involve actual wolves choruses field recorded signals [3,4]. In Experiment 2, we deal with a signal of a unique wolf howling. As expected, the signal is composed by a formant and a sequence of harmonics. Due to the background noise, only one of the harmonics has enough intensity to keep detectable. We use the noise reduction algorithm followed by the chirp separation algorithm to track and separate the formant and its harmonic. We notice that it is the fact that the chirps are separated what allow us to recognize the formant-harmonic relationship among them. Finally, in Experiment 3, we apply the separation algorithm to a very complex signal in which a chorus of an unknown number of adults and sub-adults wolves are emitting. The result of the algorithm provides a lower estimation of the number of individuals in the chorus which seems reasonable to the biologist of the team.

### *3.1 Implementation of the algorithm.*

For the numerical simulations, we use the expression of the Chirplet Transform given by (**??**). The window, $v_\lambda$, is fixed in all the experiments as a Gaussian window centered at the origin, with $\lambda = 0.1$ sec. We consider a discrete mesh of chirp rates, $\mu_m$, for $m = 1, \ldots, M$, and then, for each $m$, the discrete fast Fourier transform (**??**) is computed. Thus, we obtain the discrete Chirplet Transform $\Psi f\,(\tau_k, \xi_\ell, \mu_m, \lambda)$, with $\tau_k = \tau * k$, for $k = 1, \ldots, K$, and $\ell = 1, \ldots, L$, and with $K$ and $L$ depending on the sample frequency and the duration of the signal. The time step, $\tau$, is fixed in advance and it is related to the window overlapping in the DFFT computation. Observe that for a signal composed by $N$ samples, the number of operations is of order $\mathcal{O}\,(MN\log N)$.

According to Theorem 1, when the signal is mono-component or the various components of the signal are far from each other relative to the window width,

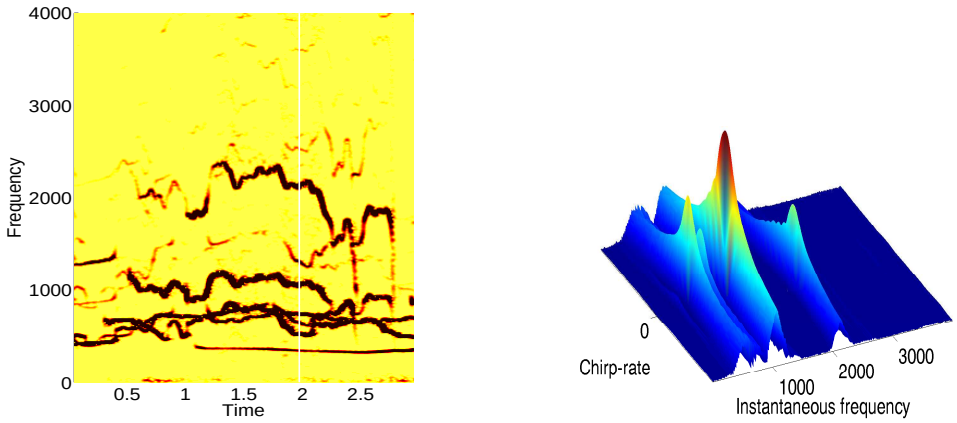


Fig. 2. Left: STFT of a field recorded signal. Right: quadratic energy distribution of the chirplet transform at $t_0 = 2$. Maxima correspond to IF and chirp rate chirps locations. We observe the different behavior in the $\xi$ and $\mu$ directions at these maxima.

the maximum of $P_\Psi f(\tau_k, \cdot, \cdot; \lambda)$ is located at some $(\xi, \mu)$ arbitraryly closed to the IF and chirp rate, $(\phi_n'(\tau_k), \phi_n''(\tau_k))$, of a chirp modulated by $\phi_n(t)$. However, when multi-component signals are close to each other or are crossing, some spurious local maxima are produced which do not correspond to any actual chirp. Therefore, some criterium must be used to select the correct local maxima at each $\tau_k$. Although we lack of an analytical proof, there are evidences suggesting that maxima produced by chirps, i.e., at points of the type $(\phi_n'(\tau_k), \phi_n''(\tau_k))$, decrease much faster in the $\xi$ direction than in the $\mu$ direction, see Fig. 2, a phenomenon that does not occur at spurious maxima. We use this fact to choose the candidates first by selecting $\xi_\ell$, for $\ell = 1, \ldots, L$, which are maxima for

$$\sup_{\mu} P_\Psi f(\tau_k, \xi, \mu; \lambda),$$

and, among them, selecting the maxima with respect to $\mu$ of $P_\Psi f(\tau_k, \xi_\ell, \mu; \lambda)$. We finally establish a threshold parameter to filter out possible local maxima located at points that do not correspond to any $\phi_n'(\tau_k)$ but which are close to two of them. We set this threshold such that the existence of two consecutive maxima is avoided. In this way we obtain, for each $\tau_k$, a set of points $(\xi_{i_k}, \mu_{i_k})$, for $i_k = 1, \ldots, I_k$, which correspond to the IF's and chirp-rates of chirps with time support including $\tau_k$.

The next step is the chirp separation. We note that if the time step $\tau$ is small enough, then

$$\xi_{j_{k+1}} - \tau \frac{\mu_{j_{k+1}}}{2} \approx \xi_{i_k} + \tau \frac{\mu_{i_k}}{2}.$$

Introducing a new parameter, $\nu$, we test this property by imposing the condition

$$\frac{1}{v} < \frac{2\xi_{j_{k+1}} - \tau\mu_{j_{k+1}}}{2\xi_{i_k} + \tau\mu_{i_k}} < \nu, \tag{8}$$

for two points to be in the same chirp. In the experiments we take $\nu = 2^{1/13} \approx 1.0548$.

Finally, in the case in which test (8) is satisfied by more than one point, i.e., when there exist points $\left(\xi_{j_{k+1}}, \mu_{j_{k+1}}\right)$ and $\left(\xi_{p_{k+1}}, \mu_{p_{k+1}}\right)$ such that (8) holds for the same $(\xi_{i_k}, \mu_{i_k})$, we impose a regularity criterium and choose the point with a closer chirp-rate to that of $(\xi_{i_k}, \mu_{i_k})$. This is a situation typically arising at chirps crossings points.

Summarizing, the chirp separation algorithm is implemented as follows:

- Each point $(\xi_{i_1}, \mu_{i_1})$, for $i_1 = 1, \ldots, I_1$, is assumed to belong to a different chirp.
- For $k = 2, 3, \ldots$, we use the described criteria to decide if $(\xi_{i_k}, \mu_{i_k})$, for : $i_k = 1, \ldots, I_k$, belongs to an already detected chirp. On the contrary, it is established as the starting point of a new chirp.
- When the above iteration is finished and to avoid artifacts due to numerical errors, we disregard chirps composed by a unique point.

Finally, once the chirps are separated, we use the following approximation, motivated by Theorem 1, to estimate the amplitude

$$a\left(\tau_k\right)^2 \approx \frac{1}{\lambda} P_\Psi f\left(t_o, \phi'\left(\tau_k\right), \phi''\left(\tau_k\right), \lambda\right),$$

for small $\lambda$.

Again, to avoid artifacts due to numerical discretization, we neglect portions of signals with an amplitude lower than certain relative threshold, $\epsilon \in (0, 1)$, of the maximum amplitude of the whole signal, considering that in this case no chirp is present.

Let us finally mention that all the experiments are performed on 16 bites–44.1 KHz sampled signals, and that typical running times on a Centrino Duo processor are in the range of minutes.

### *3.2 Experiment 1: Synthetic signals*

In this first experiment we test our algorithm with: (i) a clean synthetic signal, $f$, composed by the addition of three nonlinear chirps, and (ii) the same signal corrupted with an additive noise of similar amplitude than that of $f$, i.e., $SNR = 0$. The clean signal is given by $f(t) = \sum_{i=1}^{3} a_i(t) \cos \phi_i(t)$, for $t \in [0, 8]$, with amplitudes

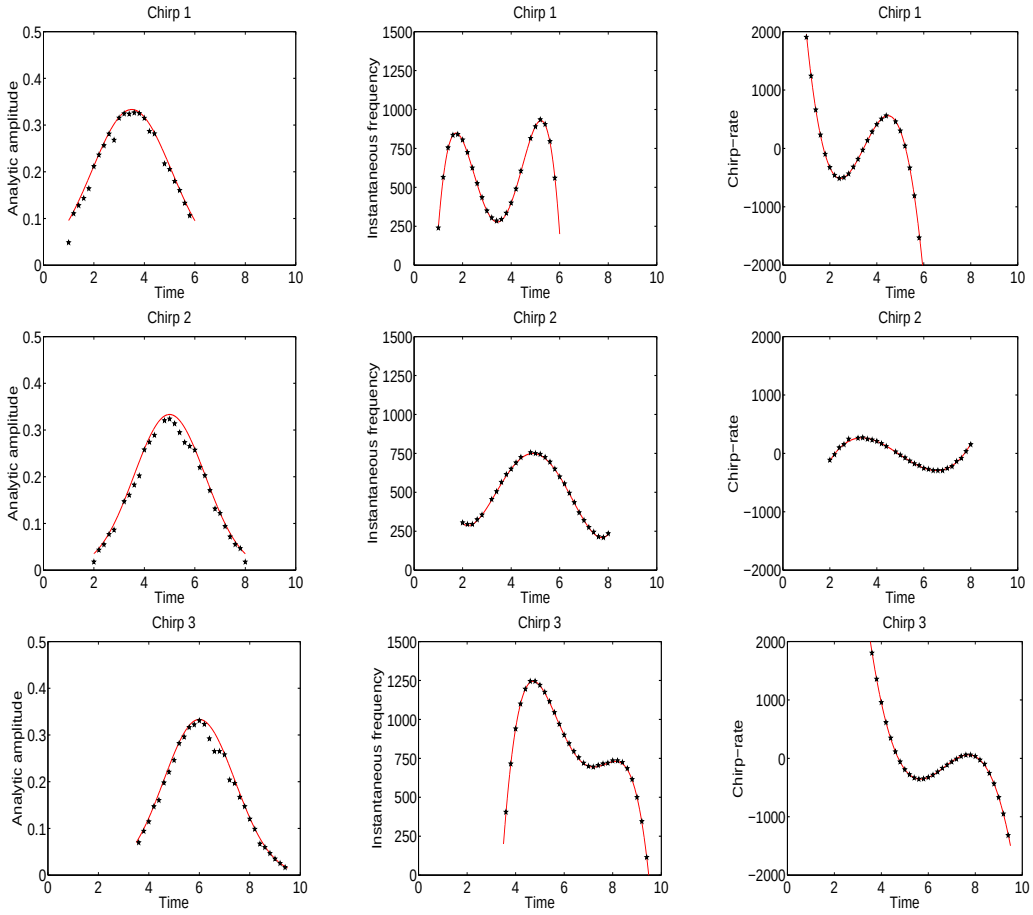


Fig. 3. Exact (solid line) and computed (dots) amplitudes, IF's and chirp rates for each voice of the clean signal of Experiment 1.

$$a_1(t) = \frac{1}{3}\exp\left(-\frac{(t-3.5)^2}{5}\right) X_{[1,6]}(t), \quad a_2(t) = \frac{1}{3}\exp\left(-\frac{(t-5)^2}{4}\right) X_{[2,8]}(t)$$

$$a_3(t) = \frac{1}{3}\exp\left(-\frac{(t-6)^2}{4}\right) X_{[3.5,6.5]}(t)$$

with $X_{[a,b]}$ denoting the characteristic function of the time sub-interval $[a,b]$, and with phases

$$\begin{aligned}
\phi_1(t) &= -13.07t^5 + 226.2t^4 - 1434t^3 + 4055t^2 - 4408t,\\
\phi_2(t) &= 1.733t^5 - 42.92t^4 + 381.1t^3 - 1459t^2 + 2798t,\\
\phi_3(t) &= -4.973t^5 + 166.3t^4 - 2172t^3 + 0.138t^2 + 0.411t.
\end{aligned}$$

We used the same time step, $\tau = 0.2$ sec, and window width, $\lambda = 0.1$ sec, to process both clean and noisy signals, while we set the relative threshold amplitude level to $\epsilon = 0.01$ for the clean signal and to $\epsilon = 0.1$ for the noisy signal. The results of our algorithm of separation are shown in Fig. 3. We

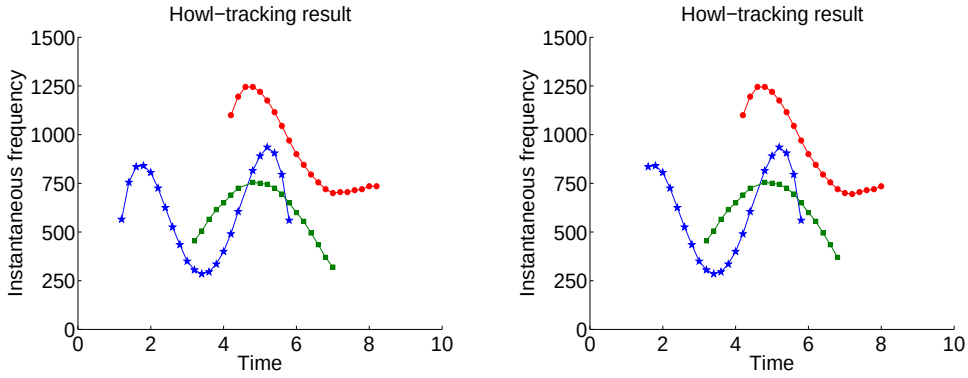


Fig. 4. Chirp separation for the noisy signal of Experiment 1 with and without previous noise filtering (left and right plots, respectively).

observe that for the clean signal all chirps are captured with a high degree of accuracy even at crossing points. However, although the number of chirps is correctly computed for the noisy signal, we observe that the main effect of noise corruption is the lose of information at chirps low amplitude range. A way to improve this result is applying the noise reduction signal enhancement algorithm described in [2] to the noisy signal and, afterwards, using the separation algorithm. As can be seen in Fig. 4, the result is somehow better than for the rough noisy signal. In Fig. 5 we show the amplitude, IF and chirp-rate estimations of the chirp which is more affected by the noise corruption, for both clean and noisy signals. The main effect of noise corruption is observed in the amplitude computation and in the lose of information at the tails of the three magnitudes.

### *3.3 Experiment 2. One wolf multi-harmonic emission*

The signal analyzed in this experiment, with STFT showed in Fig. 6, is formed by a howl of a unique individual which is composed by a formant-chirp and its corresponding harmonic chirps among which only one is detected, due to the high intensity noise level. Before using the separation algorithm, we filtered the signal to the relevant frequency band $[250, 1500]$ Hz and then applied the noise reduction signal enhancement algorithm of [2].

Parameters were fixed as follows: time step to $\tau = 0.2$ sec, amplitude threshold to $\epsilon = 0.05$ and window width to $\lambda = 0.1$ sec. The result is shown in Fig. 6. We observe that a segment of the harmonic is not detected, as expected due to the high SNR. However, the algorithm detects and separates both chirps accurately enough to perform the computation plotted in Fig. 7, showing that both chirps are harmonics and, therefore, allowing us to conclude that only one individual is emitting.

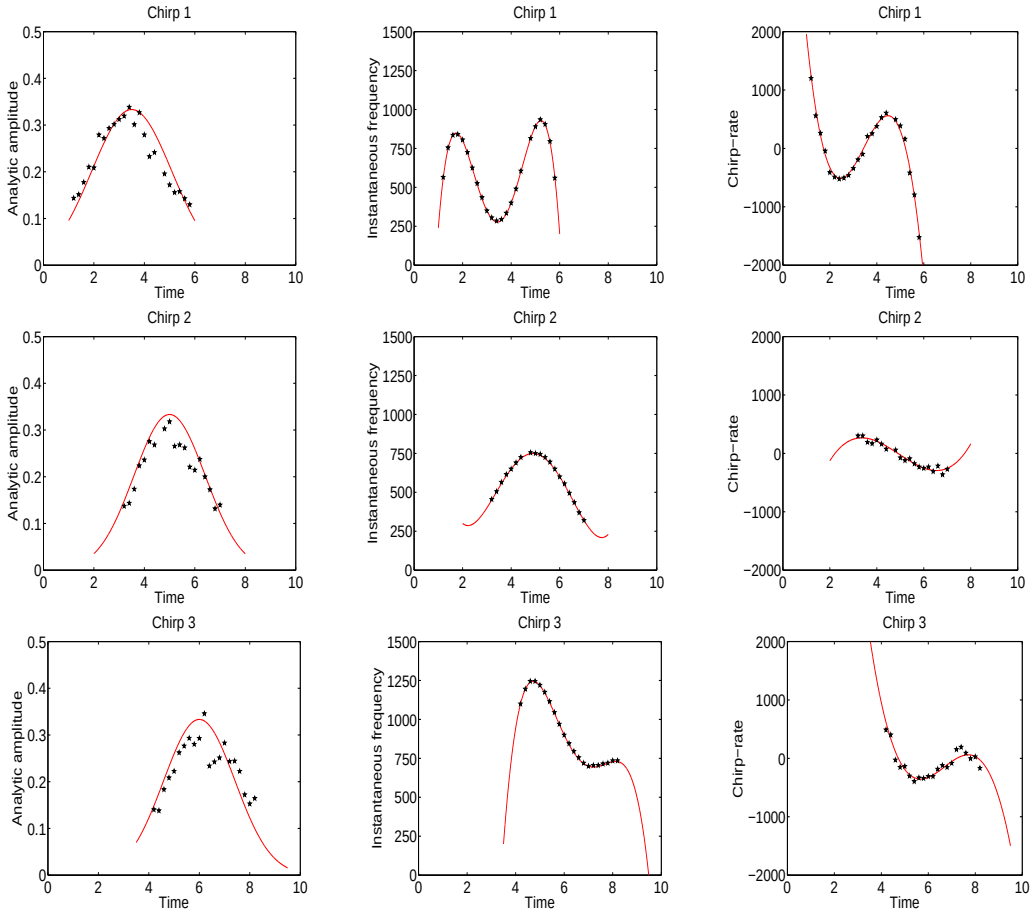


Fig. 5. Exact (solid line) and computed (dots) amplitudes, IF's and chirp rates for each voice of the filtered noisy signal of Experiment 1.

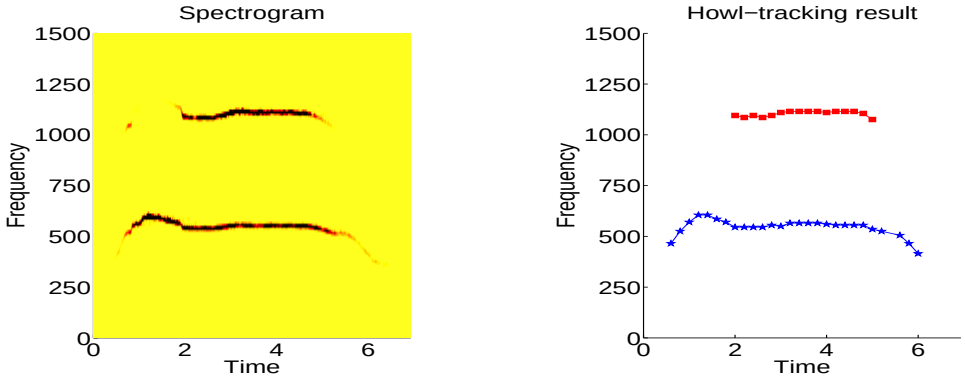


Fig. 6. Left: Experiment 2 signal's STFT. Right: Result of the separation algorithm.

### *3.4 Experiment 3. A wolves chorus*

In this experiment we analyze a rather complex signal obtained from field recordings of wolves choruses in wilderness, [3]. Due to the noise present in the recording, we first use the PDE algorithm to enhance the signal and reduce

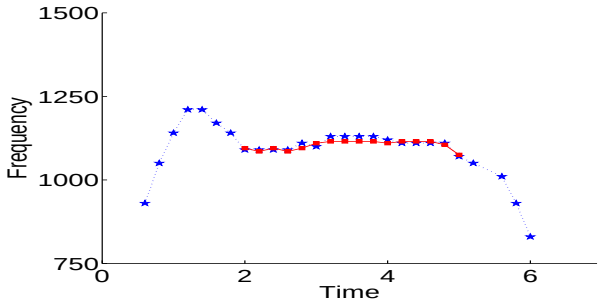


Fig. 7. The separation algorithm allows us to check the harmonicity of chirps. We plot the high frequency chirp and the diadic translation of the low frequency chirp of Fig. 6.

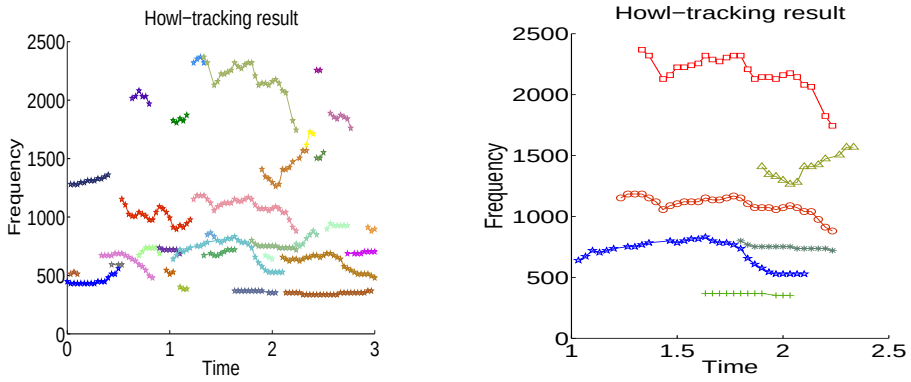


Fig. 8. Left: Result of the separation algorithm. Right: Zoom of the sub-interval $(1, 2.5)$, showing six chirps which correspond to five wolves emissions.

the noise, see [2] for details. For the separation algorithm, we fixed the time step as $\tau = 0.03$ sec, the relative amplitude threshold as $\epsilon = 0.01$ and the window width as $\lambda = 0.0625$ sec.

The output is composed by 32 chirps which should correspond to the howls and barks (with all their harmonics) emitted by the wolves along the duration of the recording. The result is shown in Fig. 1. Since our aim is giving an estimate of how many individuals are emitting in a recording, we plot a zoom of the separating algorithm result for the signals having time support at $t = 2$. Here, the number of chirps reduces to six. However, it seems that one couple of them are harmonics, the couple formed by the chirp around 1000 Hz and the chirp with highest IF. Therefore, we may conclude that at least five wolves are emitting during the interval of time plotted, $t \in (1, 2.5)$. A similar analysis may be carried out with other time slices until all the recorded signal is covered and a global lower estimate of the number of individuals is thus obtained.

## References


[1] B. Dugnol, C. Fernández, and G. Galiano. Wolves counting by spectrogram image processing. *Appl. Math. Comput.*, 186:820–830, 2007.

[2] B. Dugnol, C. Fernández, G. Galiano, and J. Velasco. Implementation of a diffusive differential reassignment method for signal enhancement. an application to wolf population counting. *Appl. Math. Comput.*, 2007. To appear.

[3] L. LLaneza and V. Palacios. Field recordings obtained in wilderness in Asturias (Spain) in the 2003 campaign. Asesores en Recursos Naturales, S.L.

[4] L. LLaneza and V. Palacios. Field recordings obtained in captivity in Spain and Portugal in the 2005 campaign. Asesores en Recursos Naturales, S.L.

[5] M. Zibulevsky and B.A. Pearlmutter. Blind source separation by sparse decomposition in a signal diccionary. *Neural Computation*, 13:863–882, 2001.

[6] L. Benaroya and F. Bimbot. Wiener based source separation with hmm/gmm using a single sensor. In *4th International symposium on Independent Component Analysis and Blind Signal Separation (ICA 2003)*, 957–961, Nara, Japan, 2003.

[7] T. Roweis. One microphone source separation. In *Advances in Neuronal Information Processing Systems (NIPS 00)*, volume 13, 2001.

[8] S. Mallat. *A wavelet tour of signal processing*. Academic Press, London, 1998.

[9] L. Stanković and I. Djurović. Instantaneous frequency estimation by using the wigner distribution and linear interpolation. *Signal Proc*, 83(3):483–491, 2003.

[10] H.K. Kwok and D.L. Jones. Improved instantaneous frequency estimation using an adaptive short-time fourier transform. *IEEE Trans. on Signal Proc.*, 48(10):2964–2972, 2000.

[11] Z. Zhao, M. Pan, and Y. Chen. Instantaneous frequency estimate for non-stationary signal. In *Fifth World Congress on Intelligent Control and Automation, 2004. WCICA 2004.*, volume 4, pages 3641–3643, 2004.

[12] B. Boashash. Estimating and interpreting the instantaneous frequency of a signal. I. Fundamentals. *Proceedings of the IEEE*, 80(4):520–538, 1992.

[13] B. Boashash. Estimating and interpreting the IF of a signal. II. Algorithms and applications. *Proc. of the IEEE*, 80(4):540–568, 1992.

[14] P. Flandrin. *Temps-fréquence*. Hermes, 1993.

[15] M. Borda, I. Nafornita, and A. Isar. New instantaneous frequency estimation method based on the use of image processing techniques. In J.T. Astola and K.O. Egiazarian, editors, *Proceedings of SPIE. Image processing: Algorithms and Systems II*, pages 147–156, 2003.

[16] S. Mann and S. Haykin. The chirplet transform: A generalization of Gabor's logon transform. *Proc. Vision Interface 1991*, 205–212, 1991.

[17] L. Angrisani and M. D'Arco. A measurement method based on a modified version of the chirplet transform for instantaneous frequency estimation. *IEEE Trans. Instrum. Meas.*, 51(4):704–711, 2002.

[18] H. M. Ozaktas, Z. Zalevsky, and M. A. Kutay. *The Fractional Fourier Transform with Applications in Optics and Signal Processing*. Wiley, Chichester, 2001.

[19] D.H. Bailey and P.N. Swarztrauber. The fractional fourier transform and applications. *SIAM Review*, 33(3):284–404, 1991.